Lab on a Chip

Accepted Manuscript

ROYAL SOCIETY OF CHEMISTRY

www.rsc.org/loc

Lab on a Chip

COMMUNICATION

Compact and modular multicolour fluorescence detector for droplet microfluidics

Russell H. Cole [a], Niek de Lange [b], Zev J. Gartner [a], and Adam R. Abate[c,†]

Received 00th January 20xx,
Accepted 00th January 20xx

DOI: 10.1039/x0xx00000x

www.rsc.org/

Multicolour fluorescence detection is often necessary in droplet microfluidics, but typical detection systems are complex, bulky, and expensive. We present a compact and modular detection system capable of sub-nanomolar sensitivity utilizing an optical fibre array to encode spectral information recorded by a single photodetector.

Droplet microfluidics enables the execution of large numbers of reactions by compartmentalizing reagents in sub-nanoliter volumes dispersed in an immiscible carrier oil.[1] The droplets can be generated,[1] injected with reagents, and sorted at kilohertz rates,[2] making them an ideal platform for high-throughput applications. Fluorescence assays are the most common readouts used in droplet microfluidics due to their bright signals, low background, and fast time response, and have been utilized for directed evolution of enzymes,[3] single cell analysis,[4] antibody screening,[5] and digital PCR.[6] While single colour fluorescence detection is sufficient for certain applications, many workflows require simultaneous measurement of multiple colours. For instance, sorting droplets based on single cell transcription[7] and evolving enzymes using *in vitro* methods[8] each require two colour detection. The standard multicolour detection approach is to filter emitted fluorescent so that each photomultiplier tube (PMT) is centered on one wavelength band. In addition to requiring multiple PMTs, this necessitates complex light filtering schemes to ensure that each PMT is optimally aligned over the desired spectral region. The use of multiple filters and detectors is expensive, difficult to miniaturize, and necessitates careful alignment of optical parts with the microfluidic channels.

Optical fibres provide an elegant solution to the challenge of achieving robust and portable droplet detection, since fibres can be integrated directly into the microfluidic device, obviating the need for further alignment, and enabling lasers and detection optics to be interfaced using simple mechanical connectors.[9,10] However, multicolour detection still requires complex light filtering and multiple PMTs, which increases cost and reduces robustness and portability. Recently, investigators have developed custom optical detection systems that utilize barcode masks to temporally encode spatial[11] and spectral[12] information on the signal recorded by a single photodetector. A system that enables multicolour droplet detection using a simplified and compact optical detection system will be a significant advance for investigators that lack the space, resources, or expertise to maintain a epifluorescence microscope based setup.

In this paper, we describe a scheme that enables multicolour detection of droplets using integrated optical fibres and a single photodetector. Optical fibres connected to lasers are inserted into the detection region at controlled, spatial offsets; another fibre connected to a photodetector monitors fluorescence at all of these regions. All fibres are aligned to the detection region using channel guides fabricated into the device, making accurate alignment simple and reliable. As droplets pass through the laser beams, multiple fluorescent bursts are generated, shifted by the amount of time for them to travel from one excitation region to the next. Because the excitations due to the lasers occur at different times, light filtering in front of the photodetector is not needed. To validate the efficacy of the detector, we quantitate fluorescence in droplet populations encapsulating dyes of different colour and concentration. To validate the approach for high throughput biological applications, we use it to detect an inhibitory antibody to matriptase, a membrane protein that is overexpressed in human cancers and an important target for drug therapies.[13] The sensitivity of the system is investigated for single colour fluorescein detection, and shows the ability to detect droplets with concentrations down to 0.1 nM, a 100X sensitivity improvement as compared to recent fibre based approaches reported in the literature [10].

[a] *Department of Pharmaceutical Chemistry, University of California, San Francisco, California, USA.*
[b] *Laboratory of Physical Chemistry and Colloid Science, Wageningen University, Wageningen, the Netherlands*
[c] *Department of Bioengineering and Therapeutic Sciences, California Institute for*Quantitative Biosciences, University of California, San Francisco, California, USA.
† Corresponding author, *email: adam.abate@ucsf.edu*

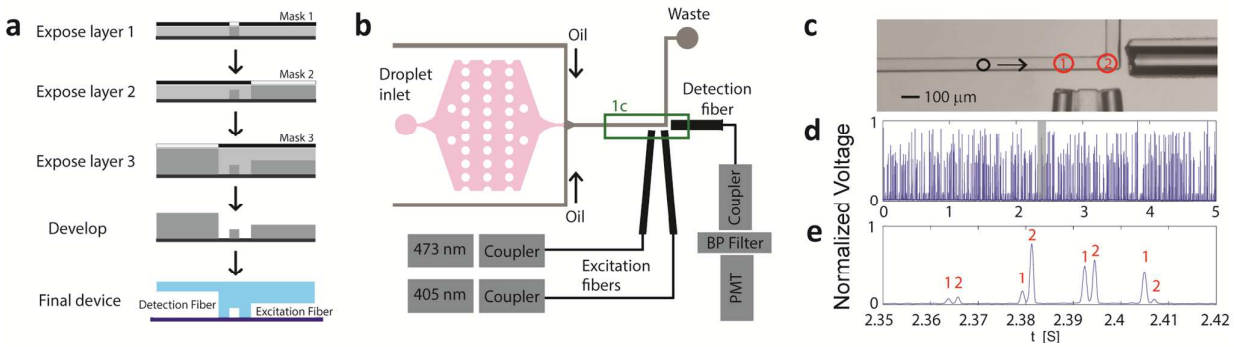

Figure 1 - (a) Three layer lithographic fabrication of the device. Three layers of SU-8 are spun on and exposed to unique masks to give a combinations of 80 µm, 120 µm, and 220 µm tall geometries for flow channels and optical fibre inserts. (b) Layout of the device, including a schematic of the fibre coupled lasers and detector. The single detector, fibre-based approach requires a bandpass filter to exclude scattered laser light, a PMT, and three optical fibres. (c) Image of the detection region of the device, where the 473 nm laser excites region "1" and the 405 nm laser excites region "2" (d) Time series for 5 seconds of acquisition (e) Time series data from a train of 4 droplets containing different dye combinations

The PDMS devices used in this study are fabricated using a photo-lithographically patterned three layer mould. Starting with a silicon wafer, an 80 µm tall layer of SU-8 3050 is spun onto the wafer, baked, and patterned with a mask to provide the fluid handling geometry (Fig 1a). Subsequently, a 40 µm tall layer of SU-8 is spun on and patterned with a 2nd mask to give 120 µm tall features, and a 100 µm tall layer of SU-8 is spun on and exposed to a 3rd mask to give 220 µm tall features. After the wafer is developed to remove unpolymerized photoresist, uncured poly(dimethylsiloxane) (PDMS) (10:1 polymer to cross-linker ratio) is poured over the photo-patterned mould. After curing in an oven at 80°C for 80 min, PDMS moulds are extracted from the masters with a scalpel and punched with access ports using a 0.75 mm biopsy core, then plasma bonded to glass slides. To render the channels hydrophobic, they are treated with Aquapel and baked at 80°C for 10 min. The tips of the optical fibres used for the experiments are stripped of their insulating layers using a stripping tool that leaves the cladding layer intact. This yields emission fibres with a cladding diameter of 125 µm, an optical core diameter of 105 µm, and a numerical aperture (NA) of 0.22. For the detection fibre, the resulting cladding diameter is 225 µm, optical core diameter 200 µm, and NA 0.39. The 125 µm fibres are coupled to lasers and the tips manually inserted into the 120 µm alignment channels parallel to the plane of the fluidic channels, accessed from the side of the device (Fig 1b). The 225 µm fibre is used to collect fluorescence because it provides a larger planar area and NA than the 125 µm fibres, and thus samples a greater proportion of the emitted fluorescence. This fibre is inserted into the 220 µm tall alignment channel and coupled to the detection optics. In between the fibre coupler and the PMT is an OD > 6 quad bandpass filter used to filter out stray laser light. The fibres are not centred on the fluid channel, so excitation and detection are not fully optimized for this particular fluidic configuration. One way to centre fibre optics on fluidic channels is by patterning complimentary features on two PDMS devices, then carefully co-locating and bonding the devices to one another, a technique that we have previously used to fabricate all PDMS co-axial flow focusing devices.[14]

Typical multicolour systems for droplet detection utilize lasers steered into the focusing objective by mirrors mounted on an optical breadboard; the emitted fluorescent light is captured by the same objective in epifluorescence mode and split off to multiple photodetectors using a series of filters and dichroic mirrors. In our lab, we have found this scheme to be problematic because of expense (epifluorescence microscopes, filters, and photodetectors are expensive), space constraints (epifluorescence microscopes and breadboard-mounted optics have significant footprints), and maintenance requirements (realignment of multiple free space lasers requires expertise). By contrast, our detection scheme reduces expense by removing the epifluorescence requirements from the microscope and reducing the filter and filter count to one each. Use of fibre optics enables a compact and modular design and makes laser alignment simple. Furthermore, including an additional colour in our scheme is as simple as adding an additional fibre mounted laser and fibre port into the device. Extending the system to perform multicolour detection on another channel requires only an additional filtered photodetector and splitting the excitation light using commercially available fibre optics splitters.

In our scheme, all colours are captured by one photodetector, shifted in time. To demonstrate that this is a viable detection strategy, we construct a microfluidic device that enables fluorescence measurement of pre-formed droplets, Fig. 1b. The device consists of a first inlet into which the droplets are introduced and a second into which oil is introduced. The droplet ejection frequency is controlled with the emulsion reinjection flow rate, while the spacing between droplets is controlled with the oil flow rate. After spacing, the droplets travel to the detection region consisting of an 80 µm channel in the shape of an "L", to which the excitation and emission fibres abut. The excitation fibres excite the regions directly opposite, denoted by the numbers "1" and "2" in Fig. 1c, while the emission fibre is oriented perpendicular to these fibres so that it can capture emitted light from both regions. As the droplets flow through the regions, they emit bursts of fluorescent light. This yields a series of doublet peaks in the time series data representative of individual droplets passing through the 473 nm and 405 nm excitation; the magnitudes of the peaks in the doublets can be tuned by adjusting the power delivered by the lasers. Time series data acquired for many droplets is shown in Fig. 1d; a close up of the data in Fig. 1e shows four unique droplet types labelled by combinations dyes that excite at 473 nm (peak 1) and 405 nm (peak 2).

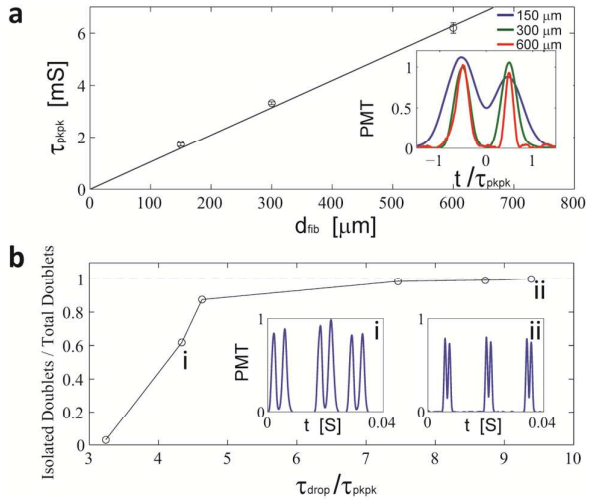

Figure 2 - (a) Measured peak-peak delay time (τ_{pkpk}) as a function of centre-to-centre fibre separation (d_{fib}). Inset gives normalized droplet signal shapes for different fibre-fibre separations. (b) The fraction of doublets from the total signal population isolated on each side by a region $2\tau_{pkpk}$ wide as a function of the normalized average droplet spacing. The insets show signal spacing data from the experiments at points marked i and ii.

Our detection scheme requires that the peaks of the doublets be clearly resolved, allowing us to confidently associate the amplitude of each peak with the intensity of light emitted for the corresponding colour channel. The clarity of the peaks depends on the separation of the excitation fibres, which we investigate by varying fibre separation (Fig. 2a). We vary the location of region 1 by moving the excitation fibre 150, 300, or 600 µm upstream of region 2; region 2 remains unaltered at 150 µm from the tip of the detection fibre. Using a flow focus droplet maker with nozzle dimensions of 60 µm in height and width, we generate ~80 µm droplets by injecting aqueous and oil at flow rates of 200 µl/hr each. The droplets consist of PBS with 10 µM fluorescein (FITC) and 10 µM 4-methyl-umbelliferone (4MU) and the oil HFE-7500 with 2% ionic Krytox surfactant.[15] They travel out of the drop maker through a 5 cm length of polyethylene tubing and into the detection device, which consists of a filter that allows the droplets to pass without splitting, and spacing junction into which surfactant-free HFE-7500 oil is introduced at 4000 µl/hr. As the droplets pass through regions 1 and 2, we observe characteristic doublets in which the temporal shift (τ_{pkpk}) between peaks is linear with fibre separation (Fig. 2a). Representative doublets for the different separations are provided inset, normalized by the average peak height and to have a temporal shift of 1. For a separation of 150 µm, the doublet peaks overlap one another due to the simultaneous excitation of the droplet by the two laser sources; this is possible because the edges of the excitation regions are only 40 µm apart, and the droplet length is 80 µm. As fibre separation is increased beyond the lengths of the droplets, the tails no longer overlap and both peaks are fully resolved, as shown by the 300 µm and 600 µm doublets in the figure. Hence, when using this detection scheme, it is important that the edges of the detection fibres be separated by more than one droplet length.

The volume fraction at which droplets can be detected is limited by the need to space them sufficiently so that the doublets of consecutive droplets are unambiguously identifiable from one another. For fixed droplet reinjection rate, the spacing between consecutive pairs of droplets depends on the oil flow rate. To illustrate this, we vary oil flow rate holding droplet flow rate constant and measure the average spacing between droplets (τ_{drop}), normalized by time between the peaks within the doublets (τ_{pkpk}).

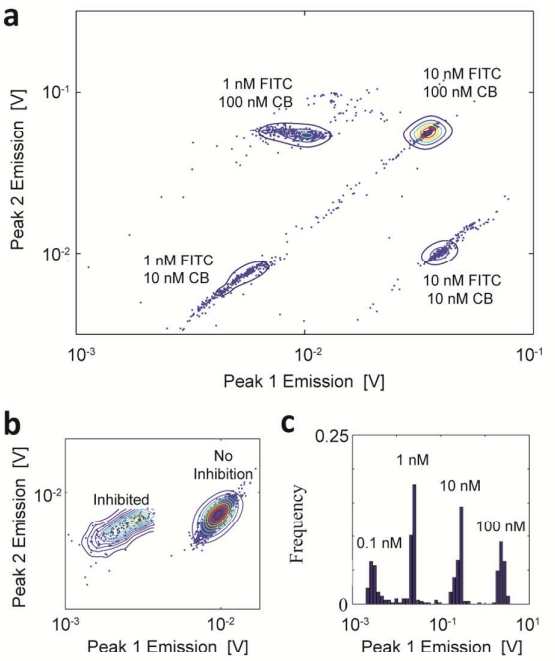

Figure 3 - (a) Scatter plot showing maximum droplet intensities for a mixed droplet population after excitation and emission by a 473 nm laser (peak 1) and a 405 nm laser (peak 2). The droplets contain combinations of fluorescein (FITC) and cascade blue (CB) at nM concentrations. (b) Scatter plot for enzyme inhibition assay. All drops contain an equal concentration of Dylight 405, making inhibited (low peak 1 emission) droplets detectable. (c) Histogram of emissions by a mixed droplet population containing 0.1 nM – 100 nM of fluorescein after excitation by a 473 nm laser.

This ratio is a non-dimensional measurement of average droplet spacing compared to the temporal shift of the doublet peaks; a value of ~4 corresponds to cases in which the average doublet spacing is comparable to the doublet size, while large values to cases in which the doublets are "narrow" compared to the space between them, and easily resolved. Droplet reinjection is somewhat aperiodic, leading to an ensemble of droplet spacings that are both smaller and larger than the average for the relevant set of flow conditions. To quantify our ability to resolve peaks, we measure the fraction of doublets that are preceded and followed by low signal regions at least $2\tau_{pkpk}$ wide and plot as a function of the normalized droplet spacing (Fig. 2b). At low values of the droplet spacing, many peaks are too close together to unambiguously associate with single droplets, resulting in only a fraction of doublet peaks being identified, as shown in Fig. 2b; a representative time series snapshot of this case is shown inset in (i), where the 2nd and 3rd doublets are separated by less than a doublet width. As spacing is increased by increasing the oil flow rate, the doublets become well separated, permitting unambiguous peak association for most doublets, as shown in (ii). Increasing τ_{drop} / τ_{pkpk} further minimally increases our ability to resolve droplets, but also increases droplet velocity; a time series snapshot for a high flow rate case is shown in (ii) inset. Since the droplet rate is maintained constant, increasing oil flow rate increases droplet velocity, resulting in proportional decreases in doublet separation and τ_{pkpk}. For this reason, the peaks for high velocities appear identical to those for low velocities, but compressed on the time axis by a value equal to the velocity ratio.

Multicolour detection is essential when performing multiplexed assays in droplets, and is often also necessary for single colour assays to count assay negative events. To characterize our detector's

effectiveness for multicolour detection, we scan droplets labelled with different concentrations of two fluorescent dyes, fluorescein (FITC) and dextran conjugated cascade blue (CB). Using flow focus droplet generation, we create four emulsions consisting of 80 μm droplets containing combinations 1nM/10nM, 1nM/100nM, 10nM/10nM, and 10nM/100nM of FITC/CB, respectively. The four emulsions are mixed, yielding a resultant mixed emulsion with multiple droplet types. We scan the mixed emulsion using the optical fibre detector. The emulsion is reinjected at 100 μl/hr, with spacer oil at 6000 μl/hr, leading to droplets passing through the detection region at ~50 Hz. We process the recorded time series data using Matlab to detect the amplitudes of the peak doublets and provide the results as scatter plot in Fig. 3a. Four distinct clusters for the different dye concentrations are observed. This demonstrates that our detector can accurately quantify droplet fluorescence for multiple channels simultaneously. In addition to strong excitation at 473 nm, FITC weakly excites at 405 nm and has the potential to affect the peak 2 emission signal; for this reason, we have chosen to use higher levels of CB dye to overcome the FITC signal at peak 2. Because emitted light is not directed to different PMTs, dyes that co-excite for the same laser wavelength cannot be individually analysed, a limitation that can be overcome by choosing dyes with adequate excitation separation. In some special cases, dyes with excitation overlap can be used if the co-excitation affects a signal that does not require sensitivity. For instance, it is often that case that applications where droplets are sorted based on a fluorescent assay utilize a secondary bright dye signal to provide a binary indicator if a droplet is present.[8,16]

Multicolour detection is important for a variety of droplet-based microfluidic screening applications, especially for analysing enzymes.[17,18] To demonstrate that our detector also performs in examples of practical importance, we use it to measure the effectiveness of a single chain variable fragment antibody inhibitor E2[19,20] for the enzyme matriptase, a transmembrane protease that is overexpressed in many cancers and is a novel therapeutic target.[13] We generate populations of 80 μm droplets containing 45 pM matriptase, 45 pM Cls substrate, 22 mM Tris buffer, 22 mM NaCl, and 2.6 nM E2 antibody fragment, as well as 1.7 μM of a 405 nm exciting fluorescent dye (Dylight 405). The substrate for matriptase is a peptide with a 5-FAM / 520 nm quencher FRET pair (C2 Cls Substrate, Anapec). As a negative control, we create a second droplet population with the same components, but in which the biologic inhibitor is not included. The emulsions take ~10 min to produce and are immediately combined at a ratio of 90% for the uninhibited and 10% for the inhibited droplets, upon which they are incubated for 2 hours at room temperature to allow the assay to progress, then detected in our device (Fig 3b). In the negative control droplets, matriptase is uninhibited and begins cleaving the substrate a soon as the droplets are formed, yielding a population of droplets that will emit fluorescence when excited at 473 nm (peak 1 emission). In the droplets containing the antibody, matriptase is inhibited, resulting in a subpopulation with low peak 1 emission. Since all droplets contain Dylight 405, all droplets give similar peak 2 emissions, enabling the detection of assay negative droplets. As expected, we observe clusters corresponding to the two populations of droplets, in which the droplets with low peak 2 emission comprise ~7.4% of all events, in reasonable agreement with the volumes in which the emulsions were combined. This demonstrates that our detector has the sensitivity to quantify the inhibition of matriptase and, likely, a variety of other enzymes with fluorescent substrates.

In order to further quantify the sensitivity of our fibre based light collection scheme, we turn off the 405 nm laser and perform single colour detection on an emulsion containing only 0.1, 1, 10, and 100 nM FITC. For these experiments, we added a second OD > 6 quad bandpass filter before the PMT to reduce noise due to scattered laser and enable 0.1 nM FITC detection. The histogram of the detected droplet intensities shows regular clusterings, separated by an order of magnitude, indicating the ability to detect down to 0.1 nM FITC, equivalent to ~17,000 molecules (2.7×10^{-20} mol) of FITC. These detection levels are comparable to those required for PCR-activated cell sorting experiments,[16] where droplets with equivalent brightness to 10^6 molecules (1.7×10^{-18} mol) of FITC need to be distinguished from baseline. The sensitivity of our detector also compares favourably to sensitivities from other fibre based approaches given in the literature – for instance, 20 nM of Alexa Fluor 488 in > 100 μm droplets.[10] This improved sensitivity is due to three factors: first, fluorescence is maximized by uniformly exciting the entire droplet volume using a > 100 μm core optical fibre to deliver laser light to the channel; second, emitted light is gathered by a fibre with a large cross sectional area and a numerical aperture similar to a standard 20X microscope objective; third, we utilize two stacked quad bandpass filters to remove more than 13 orders of magnitude of scattered laser light from the detector, greatly reducing the detector noise.

Conclusions

We have presented and characterized a multicolour detector for measuring the intensities of different spectra of light in microfluidic droplets. Our system is significantly simpler and more compact than conventional methods utilizing light filtering which require a focusing objective and multiple filters and photodetectors for different colour channels; by contrast, our system shifts the emission of different spectra in time by exciting droplets with optical fibres positioned down the length of a channel, permitting all emitted light to be captured with one photodetector. In addition to being similar in sensitivity and speed to conventional light filtering methods, our detector is compact and modular, which should enable portable fluorescent detection or simultaneous detection in parallel channels. Our detector is also compatible with droplet sorting methodologies, potentially permitting faster droplet sorting through parallelization.

Acknowledgements

This work was supported by DARPA grant number 84389.01.44908, an NSF CAREER award (DBI-1253293), an NIH exploratory/developmental research grant (CA195709), and NIH New Innovator Awards (HD080351, DP2-AR068129-01), and a New Directions grant from the UCSF resource allocation program.

References

1 S.-Y. Teh, R. Lin, L.-H. Hung and A. P. Lee, *Lab Chip*, 2008, **8**, 198–220.
2 A. Sciambi and A. R. Abate, *Lab Chip*, 2014.
3 J. J. Agresti, E. Antipov, A. R. Abate,et al., *Proc. Natl. Acad. Sci. U. S. A.*, 2010, **107**, 4004–4009.
4 L. Mazutis, J. Gilbert, W. L. Ung, D. A. Weitz, A. D. Griffiths and J. A. Heyman, *Nat. Protoc.*, 2013, **8**, 870–891.
5 B. E. Debs, R. Utharala, I. V. Balyasnikova, A. D. Griffiths and C. A. Merten, *Proc. Natl. Acad. Sci.*, 2012, 109, 11570–11575.
6 B. J. Hindson, K. D. Ness, D. A. Masquelier, et al., *Anal. Chem.*, 2011, **83**, 8604–8610.
7 D. J. Eastburn, A. Sciambi and A. R. Abate, 2013.
8 A. Fallah-Araghi, J.-C. Baret, M. Ryckelynck and A. D. Griffiths, *Lab Chip*, 2012, 12, 882.
9 M. L. Chabinyc, D. T. Chiu, J. C. Mcdonald, et al., 2001, **146**, 4491–4498.
10 F. Guo, M. I. Lapsley, A. A. Nawaz, et al., *Anal. Chem.*, 2012, **84**, 10745–10749.
11 M. Muluneh, B. Kim, G. Buchsbaum and D. Issadore, *Lab Chip*, 2014, **14**, 4638–4646.

12 J. Martini, M. I. Recht, M. Huck, M. W. Bern, N. M. Johnson and P. Kiesel, *Lab Chip*, 2012, **12**, 5057–62.
13 K. Uhland, *Cell. Mol. Life Sci.*, 2006, **63**, 2968–2978.
14 T. M. Tran, S. Cater and A. R. Abate, *Biomicrofluidics*, 2014, **8**, 016502.
15 C. Holtze, A. C. Rowat, J. J. Agresti, et al., *Lab Chip*, 2008, **8**, 1632–1639.
16 D. J. Eastburn, A. Sciambi and A. R. Abate, *Anal. Chem.*, 2013, **85**, 8016–8021.
17 J. K. Michener and C. D. Smolke, *Metab. Eng.*, 2012, **14**, 306–316.
18 C. H. Chen, M. A. Miller, A. Sarkar, et al., *J. Am. Chem. Soc.*, 2013, **135**, 1645–1648.
19 C. J. Farady, J. Sun, M. R. Darragh, S. M. Miller and C. S. Craik, *J. Mol. Biol.*, 2007, **369**, 1041–1051.
20 E. L. Schneider, M. S. Lee, A. Baharuddin, et al., *J. Mol. Biol.*, 2012, **415**, 699–715.